

Step by Step Design of a High Order Power Filter for Three-Phase Three-Wire Grid-connected Inverter in Renewable Energy System

Huang, Min; Blaabjerg, Frede; Yang, Yongheng; Wu, Weimin

Published in:

Proceedings of the 4th IEEE International Symposium on Power Electronics for Distributed Generation Systems, PEDG 2013

DOI (link to publication from Publisher):

[10.1109/PEDG.2013.6785603](https://doi.org/10.1109/PEDG.2013.6785603)

Publication date:

2013

Document Version

Early version, also known as pre-print

[Link to publication from Aalborg University](#)

Citation for published version (APA):

Huang, M., Blaabjerg, F., Yang, Y., & Wu, W. (2013). Step by Step Design of a High Order Power Filter for Three-Phase Three-Wire Grid-connected Inverter in Renewable Energy System. In *Proceedings of the 4th IEEE International Symposium on Power Electronics for Distributed Generation Systems, PEDG 2013* (pp. 1-8). IEEE Press. <https://doi.org/10.1109/PEDG.2013.6785603>

General rights

Copyright and moral rights for the publications made accessible in the public portal are retained by the authors and/or other copyright owners and it is a condition of accessing publications that users recognise and abide by the legal requirements associated with these rights.

- Users may download and print one copy of any publication from the public portal for the purpose of private study or research.
- You may not further distribute the material or use it for any profit-making activity or commercial gain
- You may freely distribute the URL identifying the publication in the public portal -

Take down policy

If you believe that this document breaches copyright please contact us at vbn@aub.aau.dk providing details, and we will remove access to the work immediately and investigate your claim.

Step by Step Design of a High Order Power Filter for Three-Phase Three-Wire Grid-connected Inverter in Renewable Energy System

Min Huang, Frede Blaabjerg, Yongheng Yang
Department of Energy Technology
Aalborg University
Aalborg, Denmark
hmi@et.aau.dk, fbl@et.aau.dk, yoy@et.aau.dk

Weimin Wu
Electrical Engineering
Shanghai Maritime University
Shanghai, China
wmwu@cle.shmtu.edu.cn

Abstract— Traditionally, when designing an *LCL*-filter, a three-phase inverter is simplified as a single-phase inverter for analysis and the output phase voltage is used to calculate the inverter-side current harmonics and to design inverter-side inductor. However, for a three-phase three-wire grid-tied system, the output current harmonics of inverter are directly affected by the output line to line voltage. Hence, this paper proposes a new method to analyze the inverter output current harmonics by using the equivalent phase voltage of the three phase inverter. Based on this, a step by step design method of the high order power filter is introduced. Simulations are carried out to verify the accuracy and the validity of the proposed methods through a 6 kW, 380V/50 Hz grid-connected inverter model with three different types of high order power filters.

Keywords—*LLCL*-filter; *LCL*-filter; current harmonics; voltage harmonics; equivalent phase voltage; design procedure; three-phase grid-tied inverter; SPWM

I. INTRODUCTION

Recently, due to the energy crisis, the distributed generation (DG) systems using clean renewable energy such as solar energy, wind energy, etc., have become an important issue in technical research. However, the use of pulse width modulation (PWM) introduces undesirable harmonics that may disturb other sensitive loads/equipment on the grid and also result in extra power losses [1]. Hence, a low-pass power filter is inserted between the voltage source inverter (VSI) and the grid to attenuate the high-frequency PWM harmonics to a desirable limit. Fig. 1 shows the structure of three-phase three-wire grid-connected inverter with different high order filters: *LCL*-filter, *LLCL*-filter with one trap [2] and *LLCL*-filter with two traps [3].

Typically, a simple series inductor L is used as the filter interface between power converters in the renewable energy system. But a high value of inductance needs to be adopted to reduce the current harmonics around the switching frequency, which would leads to a poor dynamic response of the system and a high power loss. In contrast to the typical *L*-filter, the *LCL*-filter can achieve a high harmonic attenuation performance with less total inductance ($L_1 + L_2$), significantly smaller size and cost, especially for applications above several

kilowatts [4]. In order to further reduce the total inductance even more, the *LLCL*-filter was proposed [2] and the application of the *LLCL*-filter on the three-phase three-wire Shunt Active Power Filter (SAPF) was analyzed [5]. Compared with the *LCL*-filter, the total inductance and volume of the *LLCL*-filter can be reduced which has been exemplified in a single-phase inverter. Since the voltage harmonics spectrums caused by modulation of three-phase inverter are different from that of single-phase inverter, the structure and the parameters of three-phase *LLCL*-filter should be redesigned.

Ref [3] has analyzed the character of multiple shunt *RLC* trap filters, but the detail design procedure is not given. Ref [6] presented a design procedure using the trial and error method. Some other *LCL*-filter design guidelines, criteria and optimizing processes were also proposed in [7]-[9]. However, the design principle and method of the three-phase three-wire power filter need to be further described in detail.

In this paper, the analysis on the output current harmonic of the three phase inverter using SPWM modulation methods is first presented. Secondly, a design procedure of the high order power filter is proposed and the related analysis is carried out. Finally, simulations on the designed inverter cases with three different type of high-order power filter are illustrated to verify the theoretical analysis.

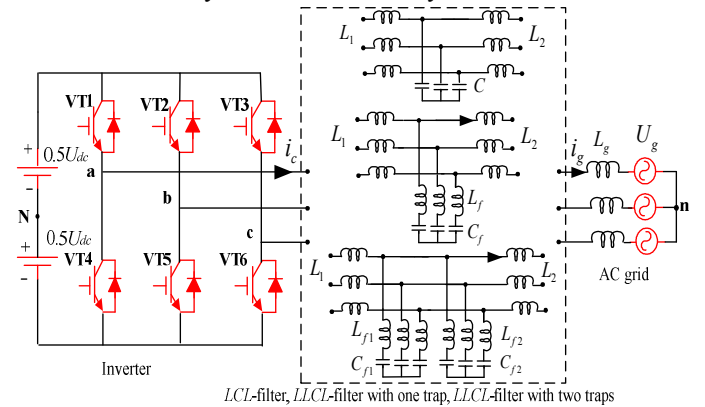


Fig. 1. Structure of three-phase three-wire inverter with different high order filters

II. INVERTER-SIDE CURRENT HARMONIC ANALYSIS FOR A THREE-PHASE INVERTER

The lower limit of the filter inductance is determined by the harmonic requirement of grid-injected current according to IEEE 519-1992[10], as specified in Table I. I_g is the nominal grid-side fundamental current. I_{SC} is the short circuit current of power system. The harmonic currents can be calculated by the corresponding harmonic voltage amplitudes at different harmonic frequencies.

TABLE I

Maximum Harmonic Current Distortion in Percent of I_g
Maximum Harmonic Current Distortion in Percent of I_g

Individual Harmonic Order (Odd Harmonics)						
I_{SC}/I_L	<11	$11 \leq h < 17$	$17 \leq h < 23$	$23 \leq h < 35$	$35 \leq h$	THD
<20	4.0	2.0	1.5	0.6	0.3	5.0

In this paper, only asymmetrical regular sampled Sinusoidal Pulse Width Modulation (SPWM) will be discussed, but the method presented can also be applied to other modulation techniques with slight modifications according to the voltage output characteristics.

A. Traditional Method

For an *LLCL*-filter or *LCL*-filter, within the low-frequency, the equivalent output impedance of the filter is approximated as the sum of the overall main inductance, while in the high-frequency range, since the capacitor bypasses the high order current harmonics, the output impedance (Z_o) of inverter is approximated as the inverter-side inductor alone [2], [7], as derived in function (1).

$$Z_o(j\omega) \cong L_1 j\omega \quad (1)$$

where L_1 is the inverter-side inductor. ω is the frequency in radians per second.

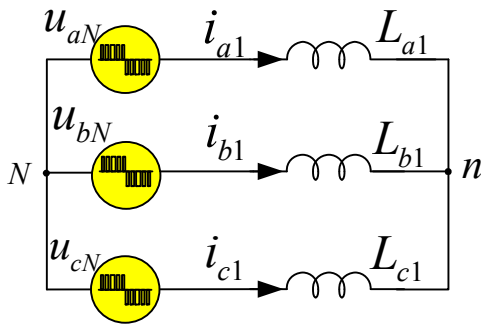


Fig. 2. Simplified three-phase voltage source inverter with phase voltage in high frequency

Traditionally, when designing a high order filter, a three-phase inverter is simplified to analyze, as shown in Fig. 2, where u_{aN} , u_{bN} and u_{cN} are three phase voltages; L_{a1} , L_{b1} and L_{c1} are converter-side inductors; i_{a1} , i_{b1} and i_{c1} are inverter-side currents in three-phase respectively. Note that the neutral point of “N” is the same as that labeled in Fig. 1.

In the SPWM mode, the amplitude of the inverter phase voltage harmonics based on the Bessel functions is given as follows [11],[12]:

$$u_{aN}(n, m) = \left| \frac{2U_{dc}}{\pi} \frac{1}{m} J_n \left(m \frac{\pi}{2} M \right) \sin \left(\frac{(m+n)\pi}{2} \right) \right|, \quad (2)$$

where

- $u_{aN}(n, m)$ amplitude of the phase voltage harmonic;
- M the modulation index;
- U_{dc} the DC link voltage;
- m carrier band number $[1, \infty)$;
- n side band number $(-\infty, +\infty)$.

When calculating the amplitude of the inverter current harmonics a three-phase three-line inverter is divided into three same single phase circuits to analyze. Usually, the amplitude of the inverter phase voltage harmonics u_{aN} is used, as shown in (3),

$$|I_{a1}|_{\omega \neq \omega_0} = \frac{|u_{aN}(n, m)|}{|Z_o(j\omega)|} \quad (3)$$

Fig. 3 shows the main harmonic current spectrum of the inverter output current under the condition that the grid-voltage (phase to phase) is 50 Hz/ 380 V, the DC-link voltage of U_{dc} is 700V, the modulation index M is 0.9, converter-side inductance L_1 is 2.4 mH and the switching frequency f_s is 10 kHz.

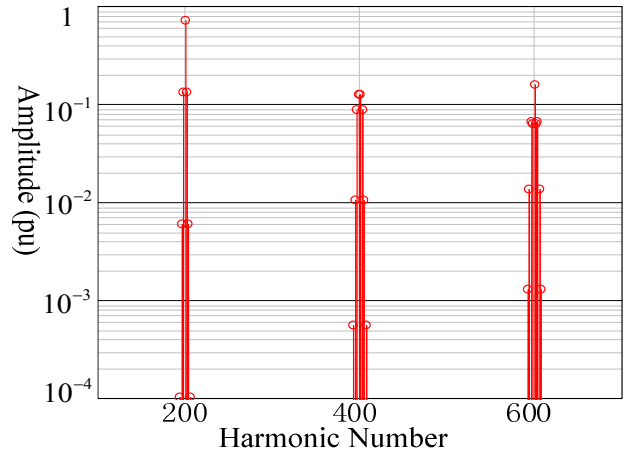


Fig. 3. Inverter output phase voltage spectrum

It can be seen output voltage harmonics around switching frequency are most significant. Then the output phase voltage harmonics can be used to obtain the current harmonics for the design of inductors. This design method is suitable for a three-phase four-wire system. But, for a three-phase three-wire system, since inverter-side point “N” (in Fig.1) is not connected to the grid neutral point “n”, the calculated harmonics of the line current using phase voltage is not so accurate.

B. Proposed Method

Considering the high-order current harmonics, Fig. 1 can be simplified as shown in Fig. 4, where u_{ab} , u_{bc} and u_{ca} are three phase line voltages, respectively.

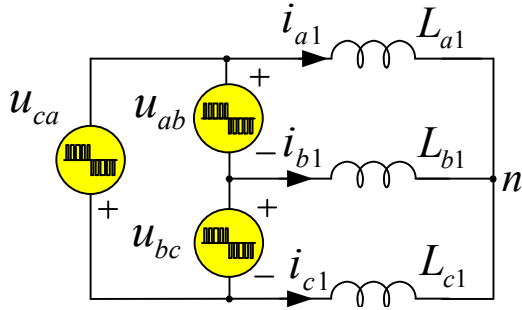


Fig. 4. Simplified three-phase voltage source inverter with line to line voltage in high frequency

According to the inverter three phase voltage functions [12], the output line to line voltage u_{ab} , u_{bc} and u_{ca} can be derived as (4):

$$\begin{aligned}
 u_{ab} &= \frac{\sqrt{3}}{2} U_{dc} M \cos(\omega_0 t + \frac{\pi}{6}) + \frac{4U_{dc}}{\pi} \sum_{m=1}^{\infty} \sum_{n=\pm 1}^{\pm \infty} \frac{1}{m} J_n \left(m \frac{\pi}{2} M \right) \\
 &\quad \cdot \sin \left[\frac{(m+n)\pi}{2} \right] \sin n \frac{\pi}{3} \cos \left[m\omega_s t + n(\omega_0 t - \frac{\pi}{3}) + \frac{\pi}{2} \right] \\
 u_{bc} &= \frac{\sqrt{3}}{2} U_{dc} M \cos(\omega_0 t - \frac{\pi}{2}) + \frac{4U_{dc}}{\pi} \sum_{m=1}^{\infty} \sum_{n=\pm 1}^{\pm \infty} \frac{1}{m} J_n \left(m \frac{\pi}{2} M \right) \\
 &\quad \cdot \sin \left[\frac{(m+n)\pi}{2} \right] \sin n \frac{2\pi}{3} \cos \left[m\omega_s t + n\omega_0 t - \frac{\pi}{2} \right] \\
 u_{ca} &= \frac{\sqrt{3}}{2} U_{dc} M \cos(\omega_0 t + \frac{5\pi}{6}) + \frac{4U_{dc}}{\pi} \sum_{m=1}^{\infty} \sum_{n=\pm 1}^{\pm \infty} \frac{1}{m} J_n \left(m \frac{\pi}{2} M \right) \\
 &\quad \cdot \sin \left[\frac{(m+n)\pi}{2} \right] \sin n \frac{\pi}{3} \cos \left[m\omega_s t + n(\omega_0 t + \frac{\pi}{3}) + \pi \right]
 \end{aligned} \quad (4)$$

where ω_s and ω_0 are the switching frequency and fundamental switching frequency in radians per second respectively. For a symmetrical three-phase circuit, three-phase line to line voltage can be converted into three-phase phase voltage, as shown in Fig. 5.

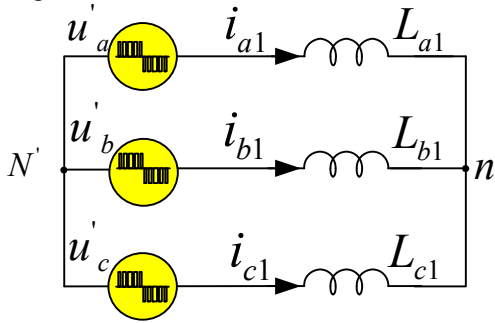


Fig. 5. Simplified voltage source inverter with equivalent output voltage sources

The equivalent phase voltage can be derived as (5):

$$\begin{aligned}
 u'_a &= \frac{u_{ab}}{\sqrt{3}} \angle -30^\circ \\
 u'_b &= \frac{u_{bc}}{\sqrt{3}} \angle -30^\circ
 \end{aligned} \quad (5)$$

$$u'_c = \frac{u_{ca}}{\sqrt{3}} \angle -30^\circ$$

Note that the neutral point of “N'” is the equivalent neutral point which is obtained from balanced three inverter-side line to line voltages and it is different from the neutral point of “N” as labeled in Fig. 1 and Fig. 2.

According to (4), the main harmonics spectrum magnitudes (p.u.) of line to line inverter output voltage by the sinusoidal pulse-width modulated waveform (SPWM) from the voltage source inverter are shown as an example in Fig. 6 under the condition that the modulation index M is 0.9 and U_{dc} is 700V.

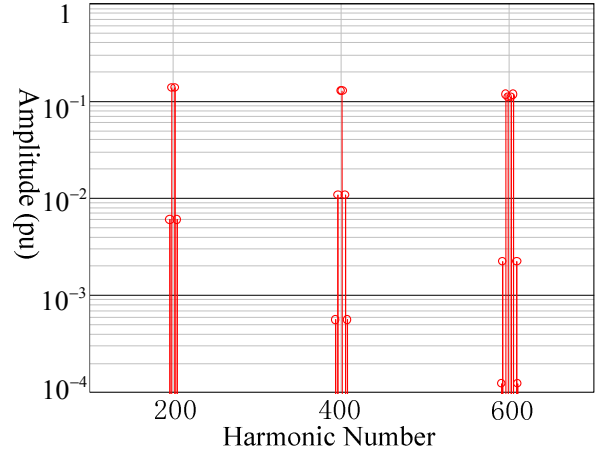


Fig. 6. Line to line output switched voltage spectrum

The amplitudes of the equivalent inverter output voltage harmonics $|U_A(n, m)|$ and the ideal amplitudes of converter-side current harmonic $|I_{AM}|$ can be derived as in (6):

$$|U_A(n, m)| = \frac{4U_{dc} J_n \left(m \frac{\pi}{2} M \right) \sin \left[(m+n) \frac{\pi}{2} \right] \sin \left(n \frac{\pi}{3} \right)}{\sqrt{3} |m\pi|}$$

$$|I_{AM}|_{\omega \neq \omega_0} = \frac{|U_A(n, m)|}{|Z_1(j\omega)|} \quad (6)$$

Since the angle does not change the spectrum of amplitude, the voltage spectrum of the equivalent phase voltage based on (5), u'_a , can also be depicted in Fig. 7.

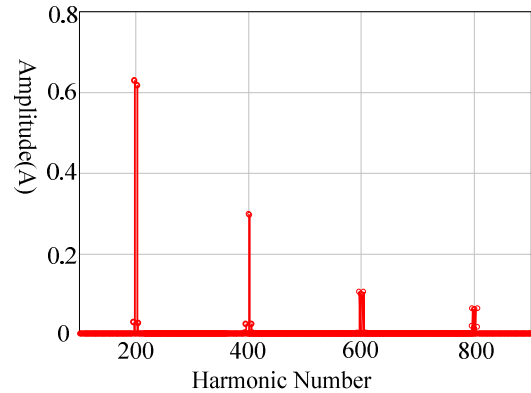


Fig. 7. The calculated harmonic spectrum of output current of inverter

With (6), the calculated harmonic spectrum of output current of inverter is shown in Fig. 7 under the condition that converter-side inductance L_1 is 2.4mH, rated power is 6 kW and switching frequency f_s is 10 kHz.

C. Simulation results of Converter-side Current Harmonics

Fig. 8 shows the simulated harmonics spectrum of the inverter-side current under the same conditions for calculation. Compared Fig. 7 with Fig. 8, it can be seen that the calculated current harmonics spectrum is almost same as the simulated current harmonics spectrum. Hence, the proposed method of equivalent output phase voltage based on line to line voltage spectrum is accurate for designing the output high order filter. It can also be seen from Fig. 8. That inverter-side current harmonics are dominant around the switching frequency and the double of the switching frequency.

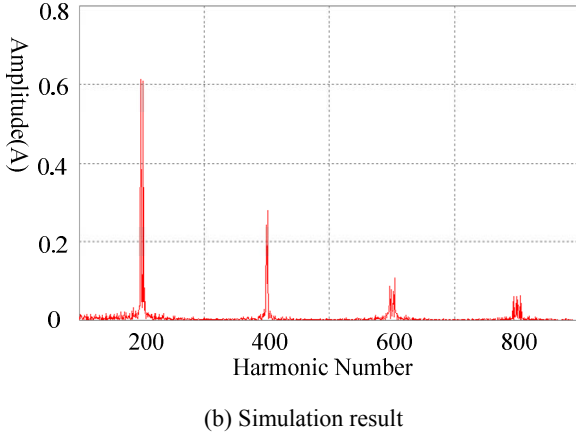


Fig. 8. Inverter-side current harmonics spectrum

III. CHARACTERISTICS OF THREE TYPICAL HIGH ORDER FILTERS

According to the converter-side current spectrum, different from single-phase inverter, the current harmonics of three-phase inverter at the double of switching are also dominant. Reference [3] makes use of multiple (n) RLC shunt trap filters, but many traps will increase the size of the filter and bring the extra cost. The *LLCL*-filter topology with two resonant circuits between the ripple inductor and the grid-side inductor to attenuate the two dominant harmonic currents around the switching frequency and the double of switching frequency can be used, as shown in Fig. 9.

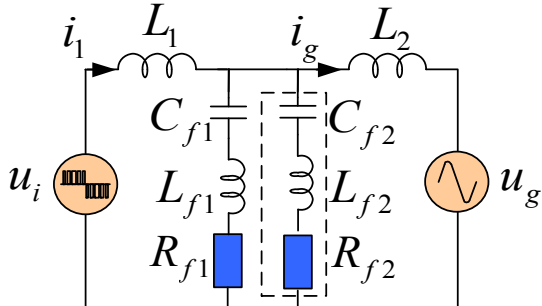


Fig. 9. Equivalent single-phase circuit of the *LLCL* filter with two traps

R_{f1} and R_{f2} is the equivalent resistor of the inductor L_{f1} and L_{f2} , respectively. Neglecting the influence of the grid impedance and equivalent series resistances (ESRs) of the inductors and capacitors, then a grid current control block diagram of the inverter with *LLCL* filter could be obtained as Fig.10.

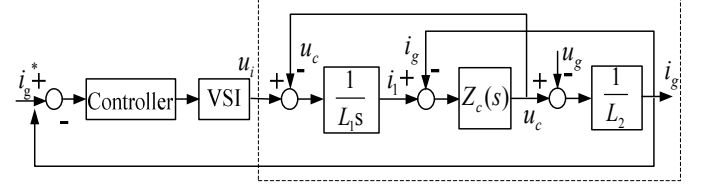


Fig. 10. Block diagram of grid current control structure with output filter

The transfer function $i_g(s) / u_i(s)$ of *LLCL*-filter with two traps can be derived as given in (7).

$$Z_1(s) = L_1 s$$

$$Z_2(s) = L_2 s \quad (7)$$

$$Z_c(s) = \frac{(L_{f1} C_{f1} s^2 + 1)(L_{f2} C_{f2} s^2 + 1)}{(L_{f1} C_{f1} C_{f2} + L_{f2} C_{f1} C_{f2}) s^3 + (C_{f1} + C_{f2}) s}$$

$$G_{u_i \rightarrow i_g}(s) = \frac{i_g(s)}{u_i(s)} \bigg|_{u_g(s)=0} = \frac{Z_c(s)}{Z_1(s)Z_2(s) + Z_1(s)Z_c(s) + Z_2(s)Z_c(s)}$$

While all the other parameters of *LCL*-filter, *LLCL*-filter with one trap and *LLCL*-filter with two traps are the same except for resonant circuits.

Fig. 11 shows the transfer functions $i_g(s) / u_i(s)$ of *LCL*-filter, *LLCL*-filter with one resonant circuit and *LLCL*-filter with two resonant circuits when L_1 , L_2 and the total capacitance are the same and the high order resonant frequencies are set at the switching frequency and the double of switching frequency.

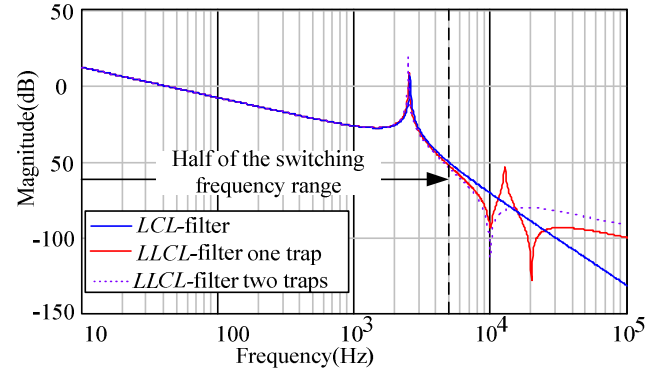


Fig. 11. Bode plots of transfer functions $i_g(s) / u_i(s)$ for different filters

From Fig. 11, it can be seen that magnitude response and phase response of the *LCL*-filter and the *LLCL*-filter in the half of the switching frequency range are similar, so there are no obvious differences during the design of the controller for *LCL*-filter and *LLCL*-filter based systems. The resonant peak

of the *LCL*-filter and *LLCL*-filter can be attenuated by same active and passive damping methods [13] - [14] and [15].

IV. PARAMETERS DESIGN OF A THREE PHASED HIGH ORDER POWER FILTER

A. Constraints on the Design of a High Order Power Filter

When designing a power filter, the base impedance of the system should be known. Then the base values of the total impedance, inductance, and capacitance are define as (8)

$$Z_b = \frac{U_n^2}{P_{rate}} \quad L_b = \frac{Z_b}{\omega_0} \quad C_b = \frac{1}{\omega_0 Z_b} \quad (8)$$

where

U_n the line-to-line RMS voltage;

ω_0 the grid frequency;

P_{rate} the active power absorbed by the converter in rated conditions.

The following aspects of the design limitation must be addressed [2] and [6]:

1) *Constrain of the total inductor (L_1+L_2)*: The maximum value of the total inductance should be less than 0.1pu to limit the ac voltage drop during operation and thereby limit the dc-link voltage.

2) *Resonance frequency of the filter*: The resonance frequency is assumed to be in a range between ten times the line frequency and one-half of the switching frequency to avoid resonance problems.

3) *Design of the filter capacitance*: It is considered that the maximum power factor variation at rated power is less than 5%, as it is multiplied by the value of base impedance of the system $C_f \leq 5\%C_b$ ($C_f = C_{f1} + C_{f2}$).

4) *The value of the inverter-side inductor (L_1)*: It is decided by the maximum ripple current.

B. Design Procedure of the High Order Filter in a Three-Phase Inverter

Based on constrains addressed above, then, the current harmonics attenuation around the triple of the switching frequency should be concentrated in the design of the three-phase three-line *LLCL*-filter design procedures can be derived as:

1) In order to meet a specific current ripple requirement, the inductance can be calculated from the equation [16]:

$$L_1 \geq \frac{U_{dc}}{8f_s(\alpha I_{ref})} \quad (9)$$

where, I_{ref} is the rated reference peak current, α is the inverter-side current ripple ratio, which generally is lower than 40% [2];

2) Select the total capacitance to achieve maximum reactive power absorbed at rated conditions.

$$(C_{f1} + C_{f2}) \leq 0.05C_b \quad (10)$$

3) Decide the resonant circuit. Since $L_{f1}-C_{f1}$ and $L_{f2}-C_{f2}$ circuit resonate at the switching frequency and the double of the switching frequency, then, L_{f1} and L_{f2} can be calculated as:

$$\frac{1}{\sqrt{L_{f1}C_{f1}}} = \omega_s, \frac{1}{\sqrt{L_{f2}C_{f2}}} = \omega_{s2} \quad (11)$$

where, ω_{s2} is twice of the switching frequency in radians per second.

4) Selection of L_2 .

For, an *LCL*-filter L_2 mainly depends on the objective to attenuate each harmonic around the switching frequency down to 0.3%. Then it can be described in (12):

$$\frac{\frac{4U_{dc}}{3\sqrt{3}\pi} \times \max\left(\left|J_2\left(\frac{\pi}{2}M\right)\right|, \left|J_4\left(\frac{\pi}{2}M\right)\right|\right) \times \left|G_{u \rightarrow g}(j\omega_s)\right|_{L_{f1,2}=0}}{I_{ref}} \leq 0.3\% \quad (12)$$

where J_2 ($1/2\pi M$) and J_4 ($1/2\pi M$) are the Bessel functions corresponding to the 2nd and 4th and the sideband harmonics at the switching frequency.

For an *LLCL*-filter with one trap based three-phase inverter, the uppermost harmonics will appear around the double of the switching frequencies.

$$\frac{\frac{4U_{dc}}{3\sqrt{3}\pi} \times \max\left(\left|J_1(\pi M)\right|, \left|J_5(\pi M)\right|\right) \times \left|G_{u \rightarrow g}(j2\omega_s)\right|_{L_{f2}=0}}{I_{ref}} \leq 0.3\% \quad (13)$$

where J_1 (πM) and J_5 (πM) are the Bessel functions corresponding to the 1st and 5th sideband harmonics at the double of the switching frequency.

For an *LLCL*-filter with two traps based three-phase inverter, the uppermost ones will appear around the triple of the switching frequency.

$$\frac{\frac{4U_{dc}}{3\sqrt{3}\pi} \times \max\left(\left|J_2\left(\frac{3}{2}\pi M\right)\right|, \left|J_4\left(\frac{3}{2}\pi M\right)\right|, \left|J_8\left(\frac{3}{2}\pi M\right)\right|\right) \times \left|G_{u \rightarrow g}(j3\omega_s)\right|}{I_{ref}} \leq 0.3\% \quad (14)$$

where J_2 ($3/2\pi M$), J_4 ($3/2\pi M$) and J_8 ($3/2\pi M$) are the Bessel functions corresponding to the 2nd, 4th and 8th and the sideband harmonics at the triple of the switching frequency.

5) Verify the resonance frequency obtained. Due to inductors L_{f1} and L_{f2} are small, the resonant frequency ω_r can be derived approximately to:

$$\omega_r \approx \frac{1}{\sqrt{\left(\frac{L_1 L_2}{L_1 + L_2}\right)(C_{f1} + C_{f2})}} \quad (15)$$

It is necessary to check resonant frequency to satisfy constraint 2). If it is not, the parameters should be re-selected from step 2).

C. Filter Design Example

Under the condition of that $f_s = 10$ kHz, $U_{dc} = 700$ V, $P_{rated} = 6$ kW, $R_{f1} = R_{f2} = 0.1\Omega$, grid phase to phase voltage is 380 V/50 Hz, and the sine-triangle, and asymmetrical regular sampled

PWM, design examples of *LCL*-filter and *LLCL*-filter are given as following:

- 1) Base on the constraint of the total inductor and inverter-side current ripple, a 28% current ripple can be obtained to design L_1 . Then the inverter-side inductor is selected to be 2.4 mH.
- 2) The total capacitor value is designed as 4 μF to limit the reactive power which should meet the constraint of 5%. Then, the capacitance of C_{f1} and C_{f2} are set to the same.
- 3) The grid-side inductor value of L_2 can be calculated by (13), (14) and (15) for three types of high order filters. In this paper, L_2 is selected to be 0.25 mH for the *LLCL* filter with two traps, 1.2 mH for *LLCL*-Filter with one trap and 2.4 mH *LCL*-filter according to functions.
- 4) For the *LC* resonant circuits, L_{f1} and L_{f2} can be chosen based on the chosen capacitors and the switching frequency.

TABLE II shows the parameters of the designed filters. Fig.11. shows the value of different inductors in three cases.

TABLE II

CONVERTER RATINGS USED FOR SIMULATIONS

Elements	Parameters	Values
Inverter	DC link voltage U_{dc}	700 V
	Switching frequency f_s	10 kHz
	Rated power P_{rate}	6kW
AC Grid	Grid phase voltage U_g	220 V
	Grid frequency f_o	50 Hz
<i>LLCL</i> -filter (two <i>LC</i> traps)	Converter side inductor L_1	2.4 mH
	Grid side inductor L_2	0.25 mH
	Resonant circuit inductor L_{f1}	128 μH
	Resonant circuit inductor L_{f2}	32 μH
	Resonant circuit capacitor C_{f2}	2 μF
	Resonant circuit capacitor C_{f1}	2 μF
<i>LLCL</i> -filter (one <i>LC</i> trap)	Converter side inductor L_1	2.4 mH
	Grid side inductor L_2	1.2 mH
	Resonant circuit inductor L_f	64 μH
	Resonant circuit capacitor C_f	4 μF
<i>LCL</i> -filter	Converter side inductor L_1	2.4 mH
	Grid side inductor L_2	2.4 mH
	Filter capacitor C	4 μF

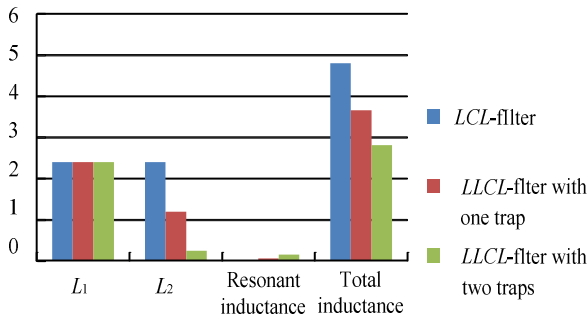


Fig. 12 Comparisons of different inductors in three cases

V. SIMULATION RESULTS

To verify the design procedure, this paper uses PI controller with voltage feed forward control. Fig. 13 shows the control block diagram of three-phase inverter system for simulation.

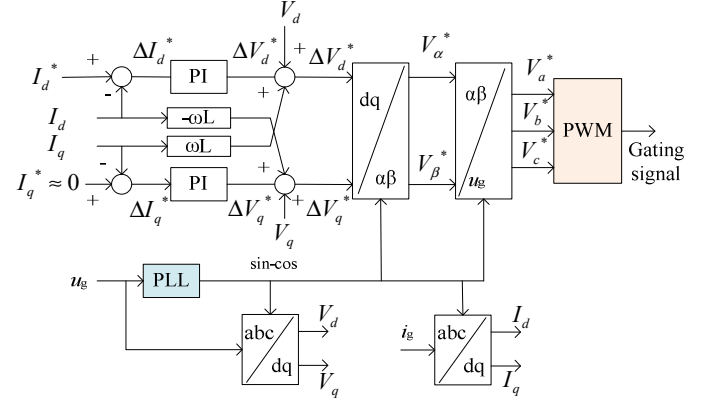


Fig. 13. Block diagram of voltage forward control of three-phase inverter

The effectiveness of the analyses is supported by simulations conducted in Matlab/Simulink and the parameters of the simulation are based on those shown in Table II. Simulation results of three cases are shown in Fig.14, Fig.15 and Fig.16 respectively.

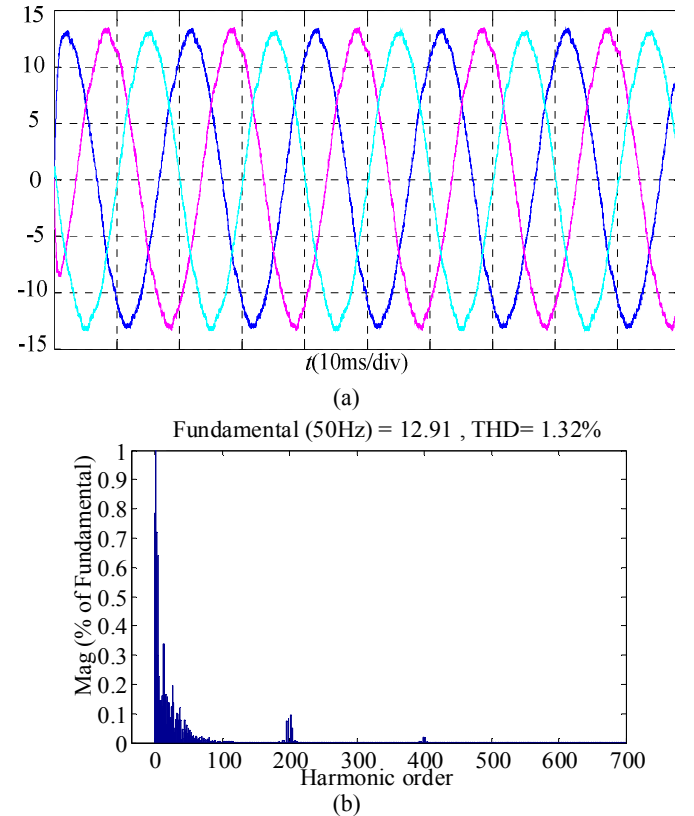


Fig. 14. Grid-side currents of *LCL*-filter based inverter. (a) Current waveforms and (b) The current spectrum.

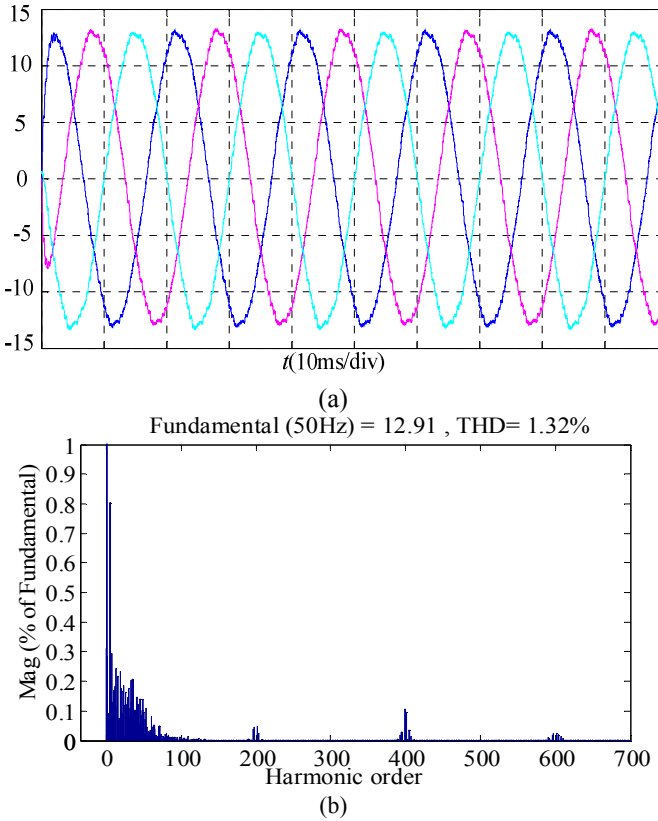


Fig. 15. Grid-side currents of *LLCL*-filter based inverter with one trap. (a) Current waveforms and (b) The current spectrum.

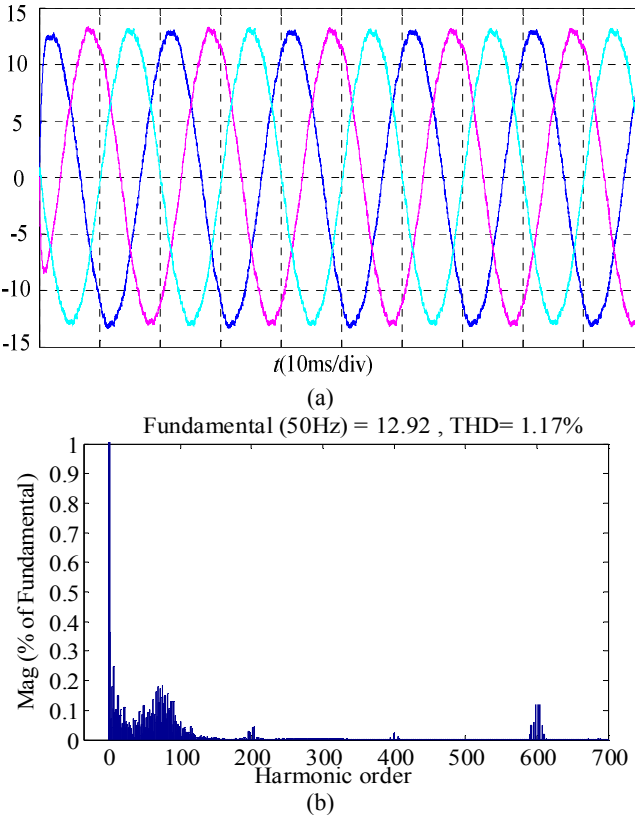


Fig. 16. Grid-side currents of *LLCL*-filter based inverter with two traps. (a) Current waveforms and (b) The current spectrum.

Fig. 14 shows the grid-side currents of *LCL*-filter based inverter which has the dominant current harmonics at the

switching frequency. Fig. 15 shows the simulated grid-side current waveforms and its spectra of *LLCL*-filter based inverter with one trap. It has most significant current harmonics at the double of the switching frequency. Fig. 16 shows that *LLCL*-filter with two *LC* traps can reduce the grid-side current ripple at the switching frequency and the double of the switching frequency.

All the design of the three case of high order based system can meet the harmonic requirement given in IEEE Standard 519-1992. Note that compared with the *LCL*-filter, the total inductance of the *LLCL*-filters with one trap and two traps can be reduced by a factor of 25% and 40% respectively.

VI. CONCLUSION

This paper has introduced a harmonic current calculation method and a step by step design method of the high order power filter in the three-phase three-wire grid-connected inverter. The following can be concluded:

1. Compared with the traditional harmonic current calculation based on the phase voltage, the proposed method based on the equivalent phase voltage is more accurate.
2. The character of *LCL* filter and *LLCL* filter in the half of the switching frequency are similar, so the additional inductor of *LLCL* filter brings no extra control difficulty.
3. Compared with the *LCL*-filter, under sine-triangle, and asymmetrical regular sampled PWM, the total inductance of *LLCL*-filters with one trap and two traps can be reduced by a factor of 25% and 40% respectively.

The accuracy of the proposed calculation on the inverter output current harmonics and the step by step parameters design method of high order filters have been verified through the simulation on a 6 kW inverter model with the current controller.

REFERENCES

- [1] H.G. Jeong, K. B. Lee, S. Choi, and W. Choi, "Performance improvement of *LCL*-filter-based grid-connected inverters using PQR power transformation," *IEEE Trans. Power Electron.*, vol. 25, no. 5, pp. 1320-1330, May 2010.
- [2] W. Wu, Y. He, and F. Blaabjerg, "An *LLCL* power filter for single-phase grid-tied inverter," *IEEE Trans. Power Electron.*, vol. 27, no. 2, pp. 782-789, Feb. 2012.
- [3] J. M. Bloemink, T. C. Green, "Reducing Passive Filter Sizes with Tuned Traps for Distribution Level Power Electronics," in *Proc. IEEE EPE 2011*, Aug. 2011, pp. 1-9.
- [4] A.A. Rockhill, M. Liserre, R. Teodorescu, P. Rodriguez, "Grid-Filter Design for a Multimegawatt Medium-Voltage Voltage-Source Inverter," *IEEE Trans. Ind. Electron.*, vol.58, no.4, pp.1205-1217, April 2011.
- [5] K. Dai, K. Duan, X. Wang, "Yong Kang Application of an *LLCL* Filter on Three-Phase Three-Wire Shunt Active Power Filter," in *Proc. IEEE INTELEC2012*, Sep. 2012, pp. 1-5.
- [6] M. Liserre, F. Blaabjerg, and S. Hansen, "Design and control of an *LCL* filter-based three-phase active rectifier," *IEEE Trans. Ind. Appl.*, vol. 41, no. 5, pp. 1281-1291, Sep./Oct. 2005.
- [7] Y. Lang, D. Xu, S. R. Hadianamrei, and H. Ma, "A novel design method of *LCL* type utility interface for three-phase voltage source rectifier," in *Proc. IEEE 36th Conf. Power Electron.*, Jan. 2006, pp. 313-317.
- [8] P. Channegowda and V. John, "Filter Optimization for Grid Interactive Voltage Source Inverters," *IEEE Trans. Ind. Electron.*, vol. 57, no. 12, pp. 4106-4114, Dec. 2010.

- [9] Limitations of Voltage-Oriented PI Current Control of Grid-Connected PWM Rectifiers with *LCL* Filters
- [10] *IEEE Recommended Practices and Requirements for Harmonic Control in Electrical Power Systems*, IEEE Standard 519-1992, 1992.
- [11] K. Jalili and S. Bernet, "Design of *LCL* Filters of Active-Front-End Two-Level Voltage-Source Converters," *IEEE Trans. Power Electron.*, vol. 56, no. 5, pp.1674-1689, May 2009.
- [12] D. G. Holmes and T. A. Lipo, *Pulse Width Modulation for Power Converters*. New York: Wiley, 2003.
- [13] W. Wu, Y. He, and F. Blaabjerg, "A New Design Method for the Passive Damped *LCL*- and *LLCL*-Filter Based Single-Phase Grid-tied Inverter," *IEEE Trans. Ind. Electron.*, vol. 60, no. 10, pp. 4339-4350, Oct. 2013.
- [14] W. Wu, M. Huang, Y. Sun, X. Wang, F. Blaabjerg, "A composite passive damping method of the *LLCL*-filter based grid-tied inverter", *In Proc. of PEDG 2012*, Aalborg, Denmark, 25-28 June 2012, pp: 759 – 766. W.
- [15] J. Dannehl, M. Liserre, and F. W. Fuchs, "Filter-Based Active Damping of Voltage Source Converters with *LCL* Filter" *IEEE Trans. Ind. Electron.*, vol. 58, no. 8, pp. 3623-3633, Aug. 2011.
- [16] T.C.Y. Wang ; Z. Ye ; G. Sinha ; X. Yuan , "Output Filter Design for a Grid-interconnected Three-phase Inverter," in *PESC '03 IEEE 34th Annual*, 2003, pp. 779 – 784.